

# Selective growth of GaN nanodots and nanostripes on 6H-SiC substrates by metal organic vapor phase epitaxy

W. H. Goh<sup>1</sup>, J. Martin<sup>2</sup>, S. Ould-Saad<sup>2</sup>, S. Gautier<sup>2</sup>, A. A. Sirenko<sup>3</sup>, A. Martinez<sup>4</sup>, L. Le Gratiet<sup>4</sup>, A. Ramdane<sup>4</sup>, N. Maloufi<sup>5</sup>, and A. Ougazzaden<sup>\*,1</sup>

<sup>1</sup> Georgia Institute of Technology/GTL - UMI 2958 Georgia Tech-CNRS, 2-3 rue Marconi, 57070 Metz, France

<sup>2</sup> Laboratoire Matériaux Optiques, Photonique et micro-nano Systèmes – UMR CNRS 7132, Université de Metz et SUPELEC, 2 rue Edouard Belin, 57070 Metz, France

<sup>3</sup> Department of Physics, New Jersey Institute of Technology, Newark, New Jersey 07102, USA

<sup>4</sup> Laboratoire de Photonique et de Nanostructures – UPR CNRS 20, Route de Nozay, 91460 Marcoussis, France

<sup>5</sup> Laboratoire d'Etude des Textures et Application aux Matériaux – UMR CNRS, 7078 Île du Saulcy, 57045 Metz cedex 1, France

Received 10 September 2008, revised 4 October 2008, accepted 27 October 2008

Published online 15 January 2009

PACS 61.05.cp, 61.46.–w, 63.22.–m, 78.30.Fs, 81.07.–b, 81.15.Kk

\* Corresponding author: e-mail aougazza@georgiatech-metz.fr, Phone: +33 03 87 20 39 23, Fax: +33 03 87 20 39 40

GaN nanodots and nanostripes with smooth sidewall surfaces have been selectively grown on 6H-SiC substrates by metal organic vapor phase epitaxy. By varying the growth reactor pressure, we have been able to grow either isolated nanostructures or laterally overgrown structures. As confirmed by the Raman scattering and X-ray diffraction techniques, the nano-

structures have no influence of step bunching that occurs in the unmasked area of the continuous GaN film. The frequency shift of the  $E_2$  optical phonons shows that the residual strain in the nanostripes is relaxed compared to the continuous GaN film.

© 2009 WILEY-VCH Verlag GmbH & Co. KGaA, Weinheim

**1 Introduction** Nanoheteroepitaxy (NHE) is a promising technique for the growth of high quality crystal structures of lattice-mismatched materials due to the three dimensional stress relief mechanisms [1]. Low dimensional systems such as nanostructured materials exhibit unique optical and electronic properties due to the carrier and photon confinement [2, 3]. Consequently, many efforts have been devoted to the growth of quantum dots, nanowires, nanorings, and nanoheteroepitaxial overgrowth of GaN and related compounds [4–8]. To date, optoelectronic and electronic devices such as quantum dot laser diodes [2], single photon sources [9] and single electron transistors [10] have been realized.

Nanoscale selective area growth (NSAG) is an advanced approach based on the combination of selective area growth and NHE, which can provide a precise control of the position and dimensions of nanostructures by using both electron-beam lithography and metal organic vapor phase epitaxy (MOVPE). Among promising applications

of NSAG are the epitaxial lateral overgrowth (ELOG) technology [11], optical microcavities, optical waveguides, photonic crystals [12], nanoscale light extraction devices, and beam directing elements for light emitting devices. Many recent activities in the NSAG field have focused on GaN nanostructure grown on GaN templates [12–14], on sapphire [13], and on Si substrates [4, 5, 8, 15], but little study has been done for the growth on 6H-SiC substrates [16]. This paper reports the growth conditions and structural properties of GaN nanodots and nanostripes grown on 6H-SiC substrates using NSAG. Comparison of the stress properties between the nanodots, nanostripes, and continuous GaN film grown on the planar substrate has been made.

**2 Experimental procedures** To fabricate a regular array of NSAG structures, a SiO<sub>2</sub> dielectric mask with a thickness of 140 nm was deposited on (0001)-oriented 6H-SiC substrates using chemical vapour deposition (CVD). After that an array of the mask openings with a diameter of

100 nm and stripes with the size of  $120 \times 7600 \text{ nm}^2$  were developed in the mask by using electron-beam lithography and reactive ion etching. These openings played a role of the nucleation sites for the GaN nanostructure growth. The GaN growth was carried out in a MOVPE T-shaped reactor [17]. The substrates were cleaned in  $\text{H}_2\text{SO}_4$  solution and then rinsed in deionized water prior to growth. Nitrogen was used as a carrier gas. Trimethylgallium (TMGa) and ammonia were used as the sources of gallium and nitrogen, respectively. The growth temperature was  $1000^\circ\text{C}$ . Two different growth pressure regimes were investigated: 100 and 450 Torr. The V/III molar ratio in the vapor phase was around 4500:1. To obtain high crystal quality and perfect selectivity, the relatively low growth rate of GaN was close to  $1\mu\text{m/h}$  in the unmasked part the wafer. The structural properties of the grown materials were characterized by x-ray diffraction (XRD), atomic force microscopy (AFM), scanning electron microscopy (SEM), and micro-Raman mapping with the lateral resolution of  $1\mu\text{m}$ .

**3 Results and discussion** Figure 1(a) shows a planar view of an SEM micrograph of the mask that was prepared for the growth of nanodots and nanostripes on a 6H-SiC substrate. One can see a regular array of nano openings with a uniform diameter of 100 nm as well as two nanostripes orientated along the  $\langle 11\bar{2}0 \rangle$  direction. The fill factor for the nanodot area, which is the ratio of the open area to the whole area of the mask, is 0.028. Figure

1(b) shows NSAG of GaN nanodots and nanostripes grown in the nano openings of the mask at 100 Torr. A perfect selectivity has been obtained at this growth condition as indicated by the absence of GaN polycrystals formed on the mask. Both the nanodots and nanostripes with smooth and homogeneous side walls are completely confined inside the mask openings.

Figure 1(c) compares higher magnification angle view SEM micrographs of the nanostructures and the continuous GaN layer grown in the non-masked area. For both growth pressures of 100 and 450 Torr, the nanodots have a much smaller height compared to the thickness of the continuous film in the non-masked area. This observation contradicts to a common expectation for the thickness enhancement in the SAG structures based on a simple gas-phase diffusion model [18]. Even in the case when the lateral size of the mask is smaller than the diffusion length  $D/k$  for precursors in the gas phase, the growth enhancement is expected in the SAG region due to formation of an excessive precursor concentration above the masked area. In the case of GaN growth,  $D/k$  is about 11 microns [19], which is comparable to the total size of the oxide mask [Fig. 1(a)]. We can see the growth enhancement regions at the edges of the continuous GaN film that surrounds the  $10 \times 10 \mu\text{m}$  mask, as expected from the gas-phase diffusion model. However, instead of enhancement for the NSAG structures, we observed significant growth rate *suppression* in both

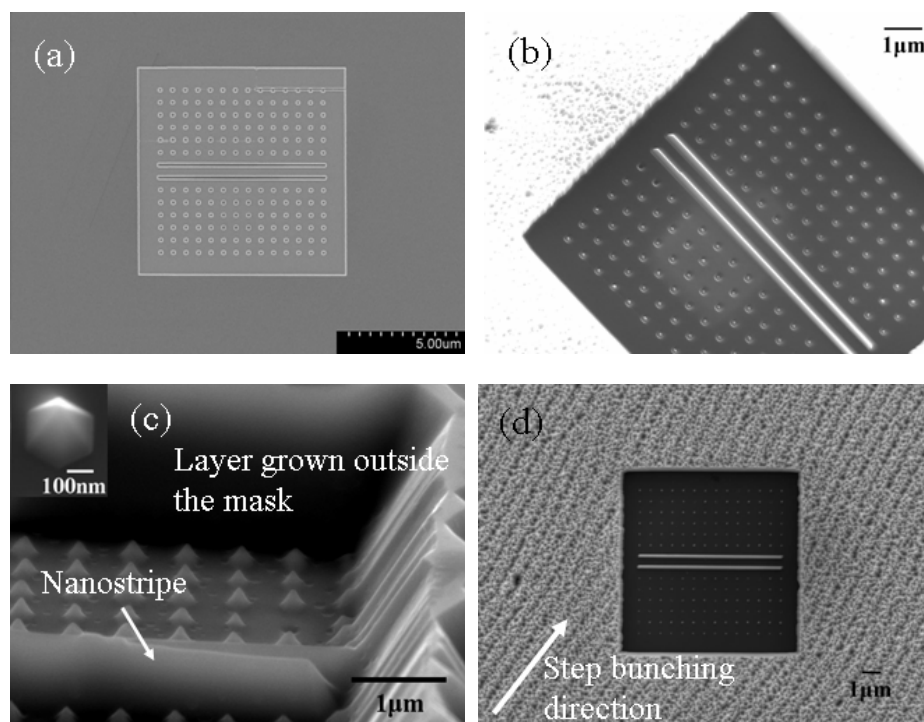


**Figure 1** (a) SEM image of the mask before growth. (b) SEM image of the nanostructures grown on SiC substrate at 100 Torr. (c) High magnification SEM angle view image of the nanostructure and the growth on the non-masked area. (d) SEM planar view image compares NSAG grown structures in the mask openings and the step bunching effect for GaN grown on the planar 6H-SiC substrate.

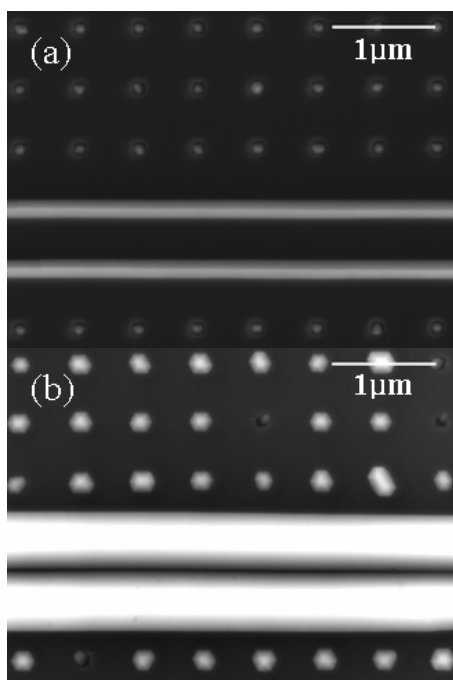
nanodots and nanostripes regions. We propose that the nucleation process inside the nano-openings is suppressed due to formation of hexagonal pyramids, which are terminated by the  $\langle 1 \bar{1} 0 1 \rangle$  facets. The growth rate at these facets is known to be much slower compared to that for the vertical growth in  $c$ -direction of GaN. In this scenario, the main factor determining the size of the dots in the NSAG region is not the fill factor of the mask, but the ratio between the nanoopening and the typical size of the nucleation grains. For the nanostripes we observed a four-times faster growth rate compared to that for nanodots, which is still much less than the growth rate for continuous film. Since one of the in-plane directions is not confined in the nanostripes, the nucleation sites can coalesce in the direction along the stripe forming a faster growing  $c$ -plane terminated facet. This mechanism eventually promotes the growth in the stripe openings compared to nanodots as it is shown in Fig. 1(c).

Figure 1(d) shows a planar view SEM image that compares the growth in the masked and non-masked areas. A self-modulated growth profile that occurred at the planar substrate (non-masked area) is due to poor wetting of Ga on SiC surface [20], which suppresses the lateral growth of GaN on SiC surface while promoting the effect of GaN bunching along the step ledges on the surface [21]. As shown in Fig. 1(d), NSAG provides a nanostripe growth along the direction determined by the mask orientation, which is not affected by the step bunching effect.

To realize the concept of ELOG on the nanoscale, the influence of growth pressure on the size and shape of the

nanostructure was investigated. Figure 2 compares SEM images of the GaN nanostructures grown at 100 and 450 Torr. At lower growth pressure, the GaN nanostructures exhibit an excellent surface morphology for the top surface, which is terminated by six smooth  $\{1 \bar{1} 0 1\}$  facets. The growth is completely confined inside the mask openings with no lateral overgrowth even for the layer thickness twice larger than that shown in Fig. 1(d). However, at high growth pressure (450 Torr), the nanostructures show epitaxial lateral overgrowth and an increase of the growth rate. The diameter of the nano pyramids grown at 450 Torr is about 3 times larger than that for the low pressure growth, as it can be seen in Figs. 2(a) and 2(b). The increase in growth rate with reactor pressure can be explained in terms of the surface migration from the mask region. The gas residence time is increased at higher pressure and, hence, more reacting species are transported to the openings before being desorbed back to the gas phase. With increase of the growth time, the nanostructures grown at high pressure will eventually coalesce together forming a high quality thin film.

A backscattering  $z(-, -)z$  Raman scanning of GaN grown in the stripe opening and on the field layer at different reactor pressure is shown in Fig. 3. In both cases the  $E_2$  phonon mode of GaN nanostripe are blue-shifted when compared with the continuous grown GaN film. The Raman intensity of the nanodots is too low and hence no comparison is made in this study. Table 1 summarizes the  $E_2$  mode frequencies and the biaxial stress determined in GaN thin film grown on planar SiC substrate and nanostripe at low and high pressure respectively. The strain-free GaN  $E_2$  mode frequency is taken to be  $567.0 \text{ cm}^{-1}$  [22]. The biaxial stress was calculated from the frequency shift by using the proportionality factor of  $4.2 \text{ cm}^{-1} \text{ GPa}^{-1}$  for wurtzite GaN [23]. The biaxial stress measured in the GaN grown on planar SiC substrate is tensile as confirmed with X-ray diffraction. The apparent relaxation of GaN thin



**Figure 2** SEM image of GaN nanostructures on SiC substrates at 100 Torr (a) and 450 Torr (b).

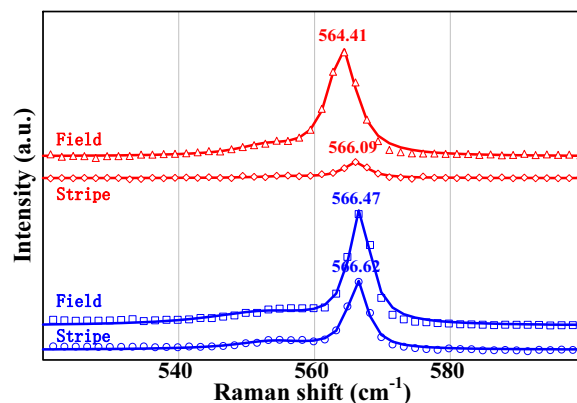


**Figure 3** Raman spectra of GaN grown in the stripe opening and on the field layer at 100 Torr (upper pairs of curves) and 450 Torr (lower pairs of curves). The symbols are experimental obtained data while the lines are curve fit of the experimental results.

**Table 1**  $E_2$  mode frequency and biaxial stress measured in GaN thin film grown in the nanostripe opening and on the planar substrate at low and high growth pressure.

Sample structure	$E_2$ frequency ( $\text{cm}^{-1}$ )	Biaxial stress (GPa)
GaN grown on planar substrate (low pressure)	564.41	-0.62
GaN grown on planar substrate (high pressure)	566.47	-0.13
GaN nanostripe (low pressure)	566.09	-0.22
GaN nanostripe (high pressure)	566.62	-0.09

film grown on planar substrate at high pressure growth as compared to low pressure could be attributed to the difference in thickness as measured by AFM (1.2  $\mu\text{m}$  for 450 Torr and 500 nm for 100 Torr). However, despite the thickness of the GaN grown on planar substrate is much more than the nanostripe [Fig. 1(c)], the nanostripes are still more relaxed than the GaN grown on planar substrate for both low and high pressure. This is due to the three dimensional stress relief mechanisms of the nanostructure [1, 24]. An average frequency shift of about 1.68  $\text{cm}^{-1}$  is observed from the nanostripe as compared to the film grown on planar substrate at low pressure which corresponds to 0.40 GPa in stress relaxation. At high pressure the  $E_2$  mode frequency is close to the strain-free GaN  $E_2$  frequency, indicating a quite complete relaxation of the residual strain in the nanostripe, which is correlated to the lateral overgrowth regime as shown in Fig. 2(b). The results indicate on one hand a relaxation of the strain inside the stripe as compared to the thin film GaN and on the other hand a relaxation of the strain for the high pressure grown thin film and nanostripe.

**4 Summary** In summary, we reported NSAG of GaN nanodots and nanostripes on SiC substrate by MOVPE. A perfect selectivity growth of the GaN has been obtained. The nanodots and nanostripes have excellent surface morphology with very smooth surface side walls. We demonstrated that our technique allows the growth of nanostripes along any in-plane crystallographic directions without any influence from the step bunching effect that occurs on the planar substrate. By varying the reactor pressure, growth of isolate nanostructures or epitaxial lateral overgrowth structures can be obtained. The lateral overgrowth nanostripes are almost completely relaxed, while the confined nanostripes are more relaxed than the GaN thin films grown on planar substrates.

## References

- [1] D. Zubia and D. Hersee, *J. Appl. Phys.* **85**, 6492 (1999).
- [2] S. Fafard, K. Hinzer, S. Raymond, M. Dion, J. McCaffrey, Y. Feng, and S. Charbonneau, *Science* **274**, 1350 (1996).
- [3] J.-Y. Marzin, J.-M. Gérard, A. Izraël, and D. Barrier, *Phys. Rev. Lett.* **73**, 716 (1994).
- [4] D. Zubia, S. H. Zaidi, S. R. J. Brueck, and S. D. Hersee, *Appl. Phys. Lett.* **76**, 858 (2000).
- [5] J. Liang, S.-K. Hong, N. Kouklin, R. Beresford, and J. M. Xu, *Appl. Phys. Lett.* **83**, 1752 (2003).
- [6] G. Kipshidze, B. Yavich, A. Chandolu, J. Yun, V. Kuryatkov, I. Ahmad, D. Aurongzeb, M. Holtz, and H. Temkin, *Appl. Phys. Lett.* **86**, 033104 (2005).
- [7] P. Chen, S. J. Chua, Y. D. Wang, M. D. Sander, and C. G. Fonstad, *Appl. Phys. Lett.* **87**, 143111 (2005).
- [8] K. Y. Zang, Y. D. Wang, S. J. Chua, and L. S. Wang, *Appl. Phys. Lett.* **87**, 193106 (2005).
- [9] P. Michler, A. Kiraz, C. Becher, W. V. Schoenfeld, P. M. Petroff, Lidong Zhang, E. Hu, and A. Imamoglu, *Science* **290**, 2282 (2000).
- [10] M. H. Devoret and R. J. Schoelkopf, *Nature* **406**, 1039 (2000).
- [11] J. Edmond, A. Abare, M. Bergman, J. Bharathan, K. L. Bunker, D. Emerson, K. Haberern, J. Ibbetson, M. Leung, P. Russel, and D. Slater, *J. Cryst. Growth* **272**, 242 (2004).
- [12] X. Wang, X. Sun, M. Fairchild, and S. D. Hersee, *Appl. Phys. Lett.* **89**, 233115 (2006).
- [13] A. Chandolu, G. D. Kipshidze, S. A. Nikishin, L. Tian, S. Daoying, M. Holtz, and A. Lobanova, *Mater. Res. Soc. Symp. Proc.* **955**, 0955-I07-14 (2007).
- [14] J. Martin, A. Martinez, W. H. Goh, S. Gautier, N. Dupuis, L. Le. Gratiet, J. Decobert, A. Ramdane, N. Maloufi, and A. Ougazzaden, *Mater. Sci. Eng. B* **147**, 114 (2007).
- [15] S. C. Lee, X. Y. Sun, S. D. Hersee, S. R. J. Brueck, and H. Xu, *Appl. Phys. Lett.* **84**, 2079 (2004).
- [16] X. Y. Sun, R. Bommena, D. Burckel, A. Frauenglass, M. N. Fairchild, S. R. J. Brueck, G. A. Garrett, M. Wraback, and S. D. Hersee, *J. Appl. Phys.* **95**, 1450 (2004).
- [17] S. Gautier, C. Sartel, S. Ould-Saad, J. Martin, A. Sirenko, and A. Ougazzaden, *J. Cryst. Growth* **298**, 428 (2007).
- [18] T. Van Caenegem, I. Moerman, and P. Demeester, *Prog. Cryst. Growth Charact. Mater.* **35**, 263 (1997).
- [19] M. E. Coltrin and C. C. Mitchell, *J. Cryst. Growth* **254**, 35 (2003).
- [20] F. R. Chien, X. J. Ning, S. Stemmer, P. Pirouz, M. D. Bremser, and R. F. Davis, *Appl. Phys. Lett.* **68**, 2678 (1996).
- [21] J. K. Jeong, J.-H. Choi, H. J. Kim, H.-C. Seo, H. J. Kim, E. Yoon, C. S. Hwang, and H. J. Kim, *J. Cryst. Growth* **276**, 407 (2005).
- [22] A. R. Goni, H. Siegle, K. Syassen, C. Thomsen, and J.-M. Wagner, *Phys. Rev. B* **64**, 035205 (2001).
- [23] C. Kiesielowski, J. Kruger, S. Ruvimov, T. Suski, J. W. Ager, E. Jones, Z. Liliental, M. Rubin, and E. R. Weber, *Phys. Rev. B* **54**, 17745 (1996).
- [24] S. Luryi and E. Suhir, *Appl. Phys. Lett.* **49**, 140 (1986).